JACS
JOURNAL OF THE AMERICAN CHEMICAL SOCIETY
pubs.acs.org/JACS



Article

# Fluorination of White Phosphorus with Fluoride Salts and Quinone Oxidants

Benjamin Falge, Maximilian Philipp, Tobias Villing, Ruth M. Gschwind, Rafael E. Rodríguez-Lugo,* and Robert Wolf*

Cite This: https://doi.org/10.1021/jacs.6c04361

Read Online

ACCESS | Metrics & More | Article Recommendations | Supporting Information

**ABSTRACT:** We report the synthesis of hexafluorophosphate ($PF_6^-$) salts directly from white phosphorus ($P_4$) and simple fluorides MF (M = Li, Na, K, Cs, $NMe_4$) in a single step. The utilization of *p*-quinones, such as 2,3-dichloro-4,5-dicyano-1,4-benzoquinone (DDQ) offers a selective fluorination pathway, which affords $MPF_6$ salts in up to 95% yield in acetonitrile (MeCN). NMR investigations of the DDQ-mediated $P_4$ fluorination reaction revealed the formation of $PF_3$ and $PF_5$·MeCN as key reaction intermediates. Donor−acceptor interactions between DDQ and fluoride are critical, effectively increasing the fluoride concentration and enabling efficient fluorination to $PF_6^-$. Tetraethylene glycol (TEG) selectively stops the reaction at the adduct K[$PF_5$·TEG]. In contrast, noncoordinating dichloromethane (DCM) favors $PF_3$ formation by suppressing EDA interactions through low fluoride solubility, possibly via the tris(hydroquinonyl)phosphite $P(DDQH)_3$, underscoring the critical role of fluoride solubility. This work demonstrates that quinone−fluoride interactions can be exploited for oxidative fluorination chemistry, establishing a new conceptual framework for $P_4$ fluorination.

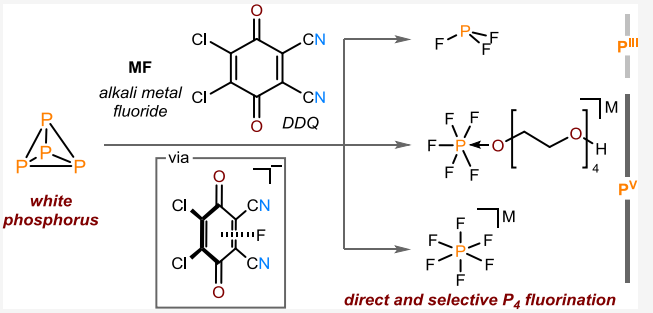


## INTRODUCTION

Fluorine imparts unique physicochemical properties due to its high electronegativity, small size, and strong element-fluorine bonds. As a result, the fluorination of organic and inorganic compounds has gained widespread importance across diverse areas of chemistry, including pharmaceuticals[1−3] agrochemicals,[4,5] functional materials,[6,7] and energy-related applications.[8]

Elemental fluorine ($F_2$) is the most powerful fluorinating agent, converting a wide range of substrates into highly fluorinated products. However, its practical use is severely limited by its hazardous nature, extreme reactivity, and poor selectivity, often leading to unselective or overoxidized products. Consequently, fluorine surrogates have been developed to enable safer and more controlled fluorination protocols.[9−13] An increasingly attractive alternative strategy involves using fluoride salts in combination with external oxidants, thereby enabling the in situ generation of electrophilic fluorinating species from simple, readily available fluoride sources.[13−15] This approach benefits from the low cost and ease of handling of inorganic fluorides such as KF or CsF, while avoiding the direct use of hazardous $F_2$. Notable examples include oxidative fluorination systems based on fluoride salts and hypervalent iodine oxidants as well as transition-metal-mediated systems in which Mn, Ni, or Ag complexes are oxidized to higher-valent fluorinating species.[16−20] In addition, electrochemistry has emerged as a powerful method for achieving fluorination under controlled conditions without the need for stoichiometric chemical oxidants.[21−23]

The fluorination of elemental phosphorus has garnered significant attention due to the crucial role of lithium hexafluorophosphate ($LiPF_6$) as a component of lithium-ion batteries.[24−31] Industrially, hexafluorophosphates are produced via the oxidation of white phosphorus ($P_4$) to $PCl_5$ using $Cl_2$ gas, followed by treatment with anhydrous hydrofluoric acid to generate phosphorus pentafluoride ($PF_5$). Reaction of $PF_5$ with metal fluorides yields the desired hexafluorophosphate salts ($MPF_6$).[32−37] Recent reports have described alternative strategies, such as the reaction of $PCl_5$ or $P_4O_{10}$ with fluorspar ($CaF_2$) at 350 °C and 1.0 MPa, followed by a reaction with LiF,[38,39] and the direct oxidation of red phosphorus ($P_{red}$) in an $F_2$ atmosphere in the presence of LiF.[40−42] Complementing these reports, Cummins and coworkers achieved the synthesis of $[nBu_4N]PF_6$ through the fluorination of $P(SiCl_3)^{2-}$, prepared from trimetaphosphate ($P_3O_9^{3-}$). This method requires $XeF_2$ as an expensive fluorinating reagent.[43,44]

Received: February 27, 2026
Revised: June 9, 2026
Accepted: June 10, 2026





https://doi.org/10.1021/jacs.6c04361
J. Am. Chem. Soc. XXXX, XXX, XXX−XXX

**Scheme 1. a) Examples of Oxidative Fluorination of Phosphorus Compounds (ref. 45−51). b) Reactivity of DDQ toward [nPr$_4$N]F, Forming DDQ$^{\bullet-}$, among Other Unidentified Products. c) Quinone-Mediated Oxidative Fluorination of P$_4$ Explored in This Work (TEG = Tetraethylene Glycol)**

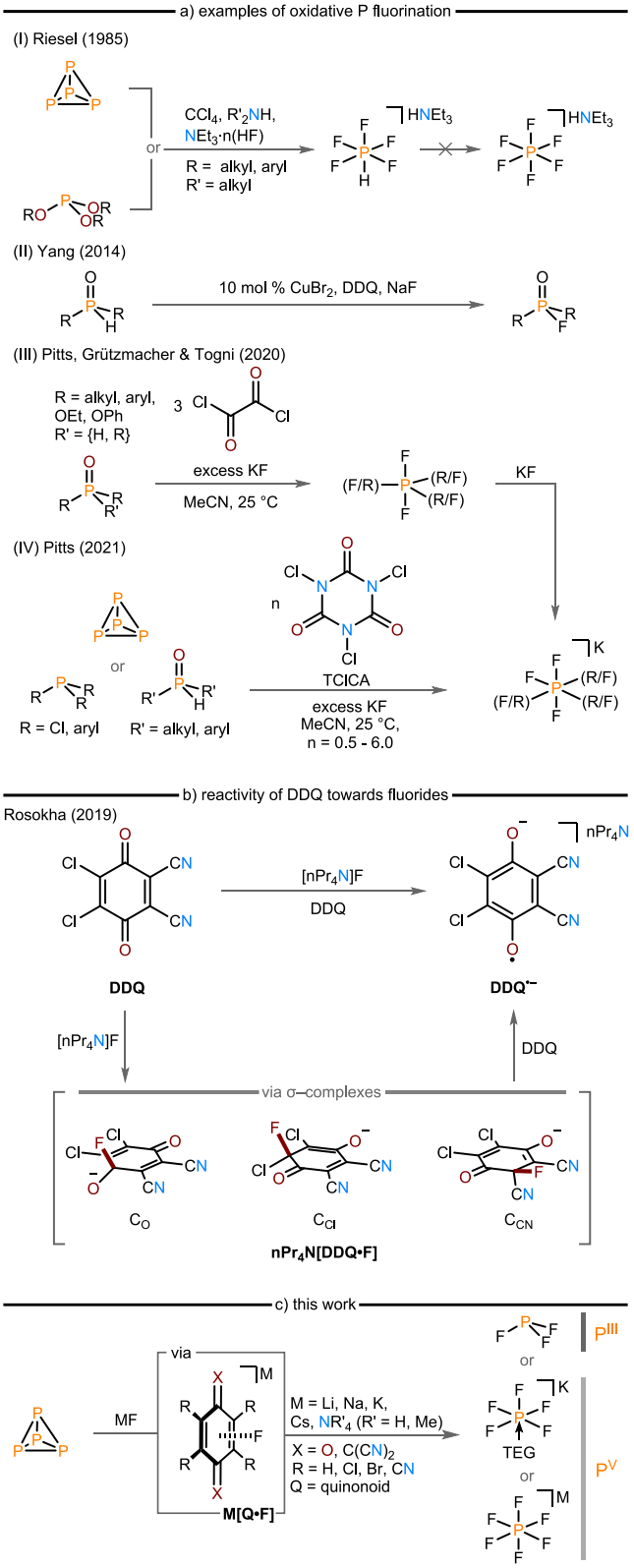


Several studies have described the fluorination of elemental phosphorus and of P(III) and P(V) compounds using a combination of oxidants and fluoride salts (Scheme 1a).[45-51] Notably, Riesel has reported that Appel-type reactions of $P_4$ and $P(OR)_3$ (R = alkyl, aryl) with $CCl_4$ and $NEt_3{\cdot}n(HF)$ (n = 1−3) afford mixtures of partially fluorinated phosphorus species, including $HPF_5^-$. However, the formation of $PF_6^-$ was not reported.[45-48] Additionally, Yang and coworkers have demonstrated the fluorination of P(V) compounds using catalytic $CuBr_2$ and DDQ as the terminal oxidant.[49] This reaction was proposed to proceed via a copper-promoted insertion of DDQ into the phosphonate P−H bond, followed by fluoride substitution. Using a different strategy, Grützmacher, Pitts, and Togni have achieved the deoxyfluorination of P(V) oxides to generate difluorophosphoranes with oxalyl chloride and KF.[50]

Notably, a subsequent report describes the oxidative fluorination of $P_4$, $P_{red}$ and P(III) compounds using trichloroisocyanuric acid (TClCA) and KF, resulting in the preparation of $KPF_6$ from $P_4$ in 62% yield.[51] Similar to classical methods, TClCA acts as a chlorine source to generate chlorinated intermediates.[52]

Despite many significant advances in $P_4$ functionalization,[53−65] the direct, one-step synthesis of hexafluorophosphates or other fluorinated phosphorus compounds from $P_4$ (or $P_{red}$) remains challenging. Rosokha and coworkers reported that DDQ and other *p*-benzoquinones form EDA complexes with fluoride. In the case of DDQ, $F^-$ anions induce the formation of the *p*-benzoquinone radical anion $DDQ^{\bullet-}$ via nucleophilic *σ*-adduct formation, followed by oxidation by a second DDQ equivalent (Scheme 1b).[66] Building on these findings, we hypothesized that combining fluoride with electron-deficient quinoids could enable $P_4$ fluorination. We now report a one-step method to synthesize hexafluorophosphates from $P_4$, inorganic fluorides, and *p*-quinonoid oxidants, which serve as both oxidants and fluoride-ion shuttles (Scheme 1c). Our studies have revealed divergent reaction pathways that provide access to intermediates such as $PF_3$ and Lewis-base-stabilized $PF_5$ adducts. The DDQ-mediated fluorination reaction has been analyzed in detail using NMR and UV−Vis spectroscopic studies, confirming that the interaction between DDQ and fluoride ions is central to the observed reactivity and directs reaction selectivity.[66]

## RESULTS AND DISCUSSION

### Reaction Discovery and Optimization

In initial experiments, we monitored the reaction of $P_4$ (0.25 equiv.) with DDQ (5.0 equiv.) in the presence of KF (7.5 equiv.) in dimethylformamide (DMF) after 18 h at 65 °C by quantitative $^{31}P\{^1H\}$ NMR spectroscopy (Table 1, SI Section S1.3). The complete conversion of $P_4$ was observed, accompanied by the formation of $KPF_6$ as the main product, in 63% yield ($\delta$ $^{31}P$ −143.8 ppm, $\delta$ $^{19}F$ −73.2 ppm, $^1J_{PF}$ = 707.0 Hz, Table S2).[67] A solvent screening showed that polar aprotic solvents like tetrahydrofuran (THF) and acetone give $KPF_6$ in low yield, although high conversions of $P_4$ are observed (Table 1). No additional species were detected by $^{31}P$ or $^{19}F$ NMR spectroscopy. The fate of the remaining phosphorus is presently unclear. Acetonitrile (MeCN), the most polar solvent tested, produced the highest yield of $KPF_6$ (95%, see Table 1, entries 1−4 and Table S2; 62% isolated yield). Ethanol led to side-product formation due to solvolysis of the fluorinated products, resulting in the formation of $OP(OEt_3)$ ($\delta$ $^{31}P$ −0.5 ppm, $^3J_{PH}$ = 8.0 Hz;




https://doi.org/10.1021/jacs.6c04361
J. Am. Chem. Soc. XXXX, XXX, XXX−XXX

**Table 1. Reaction Optimization and Control Reactions**

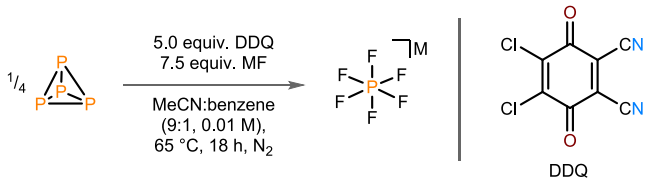


| entry | deviation from standard conditions[a] | Yield[b] |
|---|---|---|
| 1 | None: KF, MeCN, $P_4$ (0.01 M), 65 °C, 18 h, $N_2$ | 95 |
| 2 | DMF | 63 |
| 3 | Acetone | 27 |
| 4 | THF | 22 |
| 5[c] | no DDQ | n.d. |
| 6 | 25 °C | 41 |
| 7 | 25 °C, blue LED, 456 nm, 7W | 42 |
| 8 | LiF | 35 |
| 9 | CsF | 47 |
| 10 | $CaF_2$ | n.d. |
| 11 | $NMe_4F$ | 92 |
| 12 | reaction performed in air | 14 |
| 13[d] | $P_{red}$ instead of $P_4$ ($N_2$/air) | 11/22 |

[a]Standard conditions: KF, MeCN, $P_4$ (0.01 M), 65 °C, 18 h, $N_2$ atmosphere. All reactions were performed using 0.01 mmol $P_4$ (100 μL, 0.1 M in benzene). Reactions on a 0.1 mmol scale using solid $P_4$ yielded results similar to those under standard conditions ($KPF_6$: 85%, spectroscopic yield, 62% isolated yield, see SI, Sections 3.3, Figures S39–S46). [b]Yield of $MPF_6$ and conversion of $P_4$ were determined by quantitative $^{31}P\{^1H\}$ NMR spectroscopy (Figure S1). Conversion of $P_4$ in all cases >99% unless noted otherwise (Table S2). [c]No conversion of $P_4$. [d]Reaction time: 5 d.

Table S2 and Figure S2), among other nonfluorinated products.[68−70] Using dichloromethane (DCM), the reaction selectively afforded $PF_3$ ($\delta$ $^{31}P$ 104.6 ppm, $^1J_{PF}$ = 1400.9 Hz; Table S2 and Figure S3).[67] This is attributed to a different pathway operating in DCM (vide infra). Control experiments demonstrated that DDQ was essential for achieving $P_4$ fluorination (Table 1, entry 5). Irradiation with blue LED light (456 nm, 7 W) did not affect $PF_6^-$ formation (compare entries 6 and 7, Table S9).[71−74]

LiF and CsF yielded moderate amounts of the corresponding $MPF_6$ salts (35−47%; Table 1, entries 8 and 9). The yield of $LiPF_6$ did not improve upon the addition of crypt-222 (3.75 equiv.) and instead led to a less selective reaction (see Table S5 and Figures S28 and S29). Using $CaF_2$, the complete conversion of $P_4$ was observed, but no fluorinated products were detected (Table 1, entry 10). This is probably due to the poor solubility of $CaF_2$ in MeCN.[75,76] Notably, $NMe_4F$ proved to be an excellent fluoride source, affording $(NMe_4)PF_6$ in >90% yield (Table 1, entry 11). Similarly, $NEt_3{\cdot}3(HF)$, $NH_4F$, and $KBF_4$ gave the corresponding $MPF_6$ salts in yields ranging from 27% to 73% (Table S5).[77] The reaction is sensitive to oxygen and moisture. When the reaction was carried out in air, $KPF_6$ was obtained in low yield (14%), alongside $KPO_2F_2$ (Table 1, entry 12, $\delta$ $^{31}P$ −17.9 ppm, t, $\delta$ $^{19}F$ −82.9 ppm, d, $^1J_{PF}$ = 957.7 Hz; SI Section S3.1).[67,68] $P_{red}$ can also be fluorinated, affording $KPF_6$ in low yields when the reaction is performed in air or under an $N_2$ atmosphere (22% and 11% yield, respectively; Table 1, entry 13, Figures S36–S38). These results indicate that an inert atmosphere is mainly necessary to mitigate premature oxidation of $P_4$ by air.

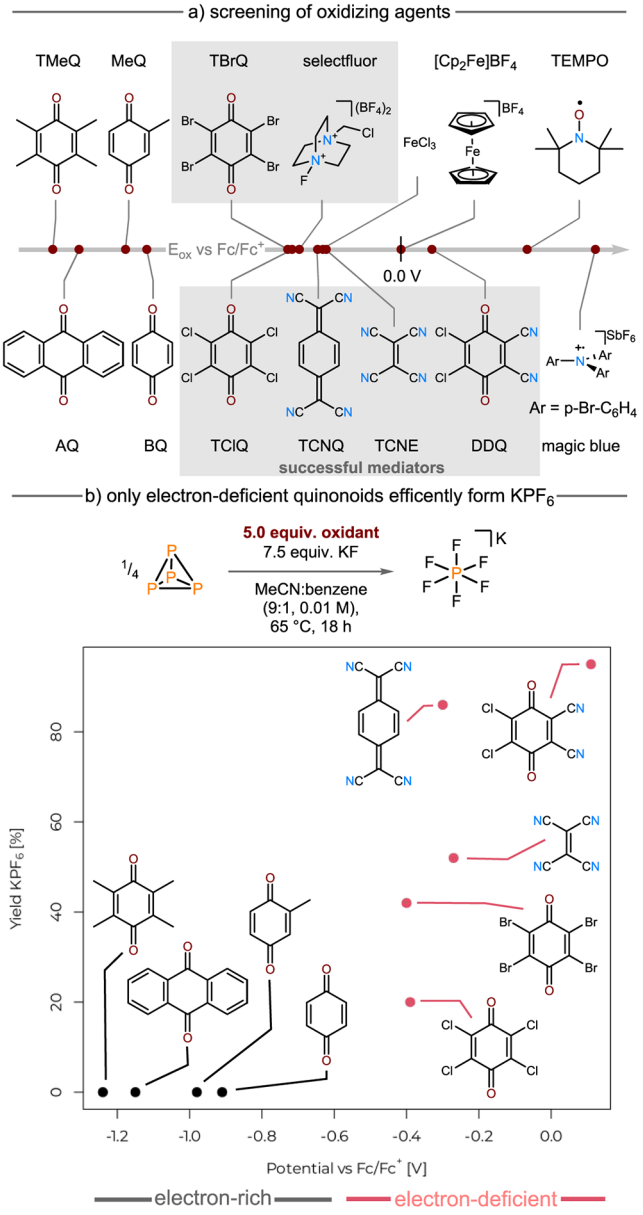


**Figure 1.** Impact of selected oxidants on $P_4$ fluorination reaction. a) Structures and oxidation potential ($E_{1/2}$ vs $Fc/Fc^+$ in MeCN) of some selected oxidants used. Successful mediators highlighted in gray. b) Scatter plot showing the yield of $KPF_6$ against oxidation potential for *p*-quinonoids in the $P_4$ fluorination reaction.

## Impact of Oxidizing Agents

To investigate the role of the oxidant in this transformation, we evaluated various electron acceptors in the fluorination of $P_4$ to $KPF_6$ (Figure 1a, Tables S7–S10).[78,80] No general correlation of product yield with formal half-wave potentials ($E_{1/2}$ vs $Fc/Fc^+$ in MeCN) of the oxidants was found. For example, TCNQ ($E_{1/2}$ = −0.30 V) and TCNE ($E_{1/2}$ = −0.27 V)[78,81] both enabled productive conversions, whereas TEMPO ($E_{1/2}$ = 0.26 V)[82] gave full conversion of $P_4$ but did not result in any fluorination, despite having a significantly higher oxidation potential. This shows that reactivity is not solely governed by oxidation power. Inspection of the mediators that successfully produced $KPF_6$ reveals that most of them contained a *p*-quinonoid moiety (Figure 1b). It is important to note, however, that electron-rich quinones failed to produce $KPF_6$ (Tables S7–S9).[79,80,83] $KPF_6$




https://doi.org/10.1021/jacs.6c04361
J. Am. Chem. Soc. XXXX, XXX, XXX−XXX

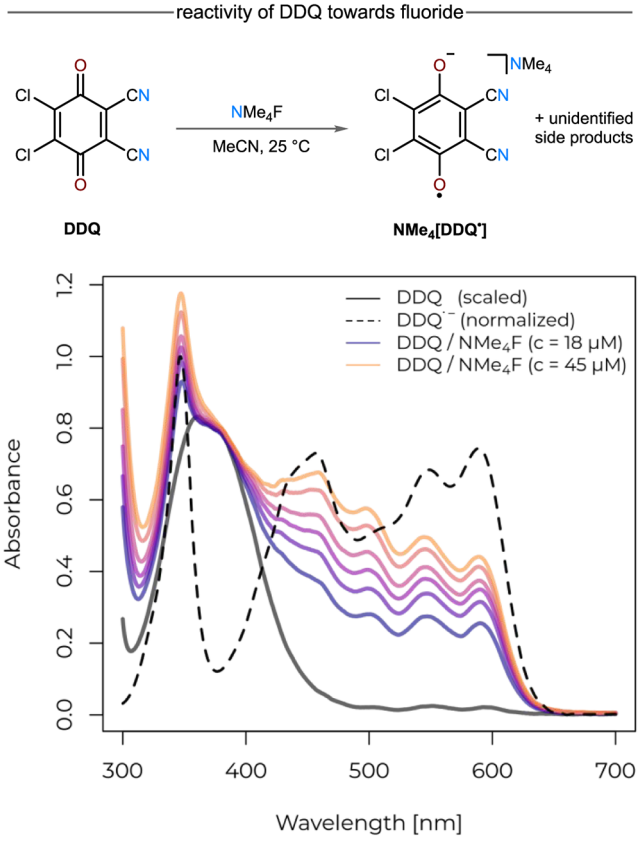


**Figure 2.** UV−Vis titration of DDQ (0.91 mM in MeCN) with $NMe_4F$, showing the formation of $DDQ^{\bullet-}$. Normalized and scaled data were obtained from spectroelectrochemistry of DDQ (see SI, Section S3.6).

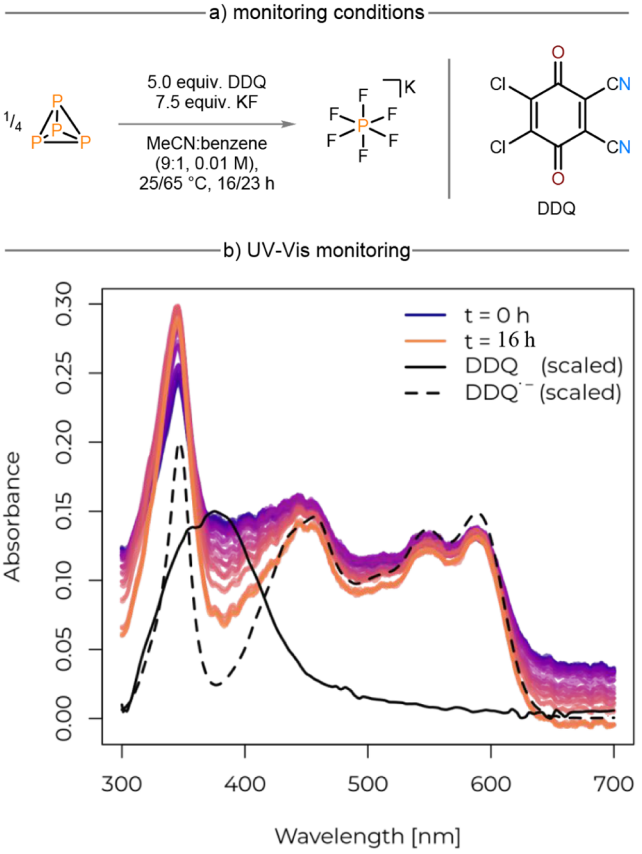


**Figure 3.** a) Conditions of the in situ reaction monitoring studies. b) UV−Vis reaction monitoring of a dilute reaction solution over 16 h at 25 °C, showing the consumption of DDQ and formation of $DDQ^{\bullet-}$. No $DDQ^{2-}$ was detected. For details, see SI Section S3.6 and S3.18.

formation is seen only with quinoids that have an oxidation potential of at least −0.4 V vs $Fc/Fc^+$. As a result, DDQ, the strongest commercially available quinonoid oxidant ($E_{1/2}$ = 0.13 V), achieved the highest yield (95%).[80]

## Studies on the Role of DDQ

Quinonoid compounds participate in electron donor-acceptor interactions with a range of donors, including halides and pseudohalides.[66,84−87] Rosokha and coworkers previously proposed that the reduction of DDQ occurs via transient $nPr_4N[DDQ{\cdot}F]$ $\sigma$-complexes, formed by fluoride addition to electrophilic positions on the quinone ring ($C_O$, $C_{Cl}$, or $C_{CN}$; Scheme 1b).[66,84,88] These intermediates, possessing higher HOMO energies relative to DDQ, are susceptible to single-electron oxidation by a second equivalent of quinone, forming $DDQ^{\bullet-}$.[66,89,90] To investigate whether similar complexes form under our reaction conditions, we added fluoride salts (MF) to solutions of DDQ in MeCN and monitored the solutions by UV−Vis absorption spectroscopy. The resulting immediate color change from orange to deep purple suggested transient formation of a fluoride-DDQ complex. Upon treatment of DDQ (Figure 2, black line, 0.91 mM, 1.0 equiv.) with substoichiometric $NMe_4F$ (0.018−0.045 mM, 0.02−0.05 equiv.) in MeCN, the absorption spectra (Figure 2, colored lines) revealed the characteristic absorptions of $DDQ^{\bullet-}$ (Figure 2, black dashed line), suggesting that DDQ is reduced under these conditions (via the pathway shown in Scheme 1b).[66]

$^{19}F\{^1H\}$ NMR monitoring of the reaction between DDQ and KF at 65 °C gave an intractable mixture showing a large number of unidentifiable signals (Figure S67), which may possibly arise from the fluorination of DDQ. Since fluoride salts are generally poorly soluble in MeCN,[75] we presume that the interaction between DDQ and fluoride plays a crucial role in increasing the fluoride concentration. This is in line with the observed reactivity trend among quinonoid oxidants, which all possess electron-deficient $\pi$-systems.[91] In contrast, oxidants that failed to promote fluorination typically possess more electron-rich cores (e.g., *p*-benzoquinone, Figure 2) or do not readily act as fluoride acceptors (e.g., TEMPO). As a result, these reagents oxidize $P_4$ without facilitating fluoride transfer, leading to unproductive reaction pathways.

UV−Vis monitoring of the reaction between DDQ and $P_4$ in the absence of fluoride reveals no significant changes in the visible region, indicating that no EDA complex forms in this case (SI Section S3.8). In contrast to the rapidly developing $DDQ^{\bullet-}$ signal upon fluoride addition (Figure 2), no accumulation of $DDQ^{\bullet-}$ was observed. Instead, very weak bands assigned to $DDQ^{\bullet-}$ disappeared completely within 3 days (Figures S13−S16). It is important to note that the reaction between DDQ and fluoride occurs very fast after mixing both reagents. Although largely dependent on fluoride solubility (vide infra), it is significantly faster than the reaction of DDQ or $DDQ^{\bullet-}$ with $P_4$.

To further gain insight into the role of DDQ, we monitored the reaction of $P_4$ and DDQ in the absence of fluoride by $^{31}P\{^1H\}$ NMR spectroscopy in MeCN-$d_3$/$C_6D_6$ (9:1, v:v, see Scheme 2 and Figure S61). Heating at 65 °C for 18 h resulted in 58% conversion of $P_4$ and a new resonance at $\delta$ $^{31}P$ 136.1 ppm, assigned to the tris(hydroquinonyl)phosphite, $P(DDQH)_3$,




https://doi.org/10.1021/jacs.6c04361
J. Am. Chem. Soc. XXXX, XXX, XXX−XXX

**Scheme 2. Reactivity of DDQ and K[DDQ$^{\bullet}$] toward $P_4$ and Further Reactivity with KF in Deuterated Solvents**

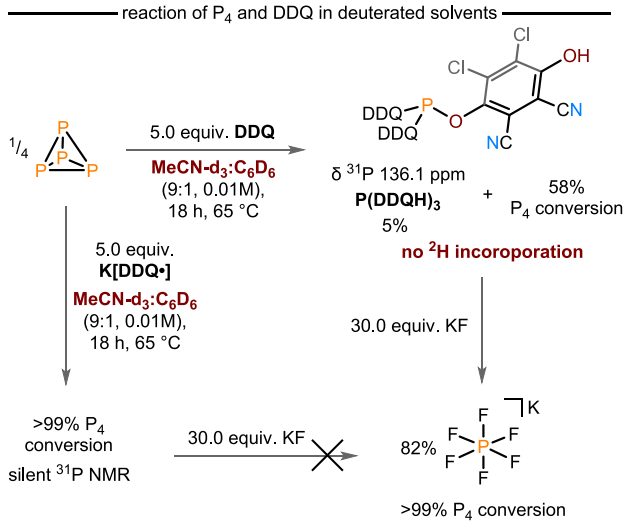


which was formed in 5% yield, as determined by $^{31}P\{^1H\}$ NMR integration. The assignment is based on reported resonances of related phosphites (e.g., $P(OPh)_3$: $\delta$ $^{31}P$ 126 ppm).[58] We propose that these hydroquinonyl units are protonated, based on control experiments which showed that $DDQH_2$ (1.0 equiv.), upon deprotonation with NaH followed by addition of $PCl_3$ (0.33 equiv.), gave the same major $^{31}P\{^1H\}$ NMR signal ($\delta$ 136.1 ppm, Figure S58). The protons presumably originate from traces of moisture and not from the solvents MeCN-$d_3$ or $C_6D_6$, as no signals for deuterated OH groups were detected by $^2H$ NMR spectroscopy (Figures S59 and S60). Subsequent addition of KF (7.5 equiv.) to the same reaction mixture afforded $KPF_6$ in 82% yield, with full consumption of $P_4$ and $P(DDQH)_3$ (Figures S62 and S63). These observations demonstrate that $P(DDQH)_3$ is only a minor intermediate and suggest that other NMR-silent phosphorus species[92] are present that are also chemically active in the fluorination reaction (Scheme 2).

Treatment of K[DDQ$^{\bullet}$] (5.0 equiv.) with $P_4$ (0.25 equiv.) in MeCN-$d_3$ at 65 °C for 18 h resulted in the complete consumption of $P_4$. No other signals were detected in the $^{31}P\{^1H\}$ NMR spectrum of the reaction mixture (Figure S64). Performing the same reaction in the presence of KF resulted only in traces of fluorination products, indicating that K[DDQ$^{\bullet}$] oxidizes $P_4$, but the resulting phosphorus compounds do not participate in the fluorination reaction (Figures S65 and S66).

## In Situ Reaction Monitoring

To further understand the reaction pathways, we monitored the reaction of $P_4$ with DDQ and KF in situ by UV−Vis and $^{31}P\{^1H\}$ NMR spectroscopy. UV−Vis monitoring revealed that DDQ is converted into $DDQ^{\bullet-}$ (Figure 3), confirming that DDQ acts as a one-electron acceptor in this reaction. Absorption bands associated with $DDQ^{2-}$ were not detected (Figures S8, S10 and S21, S22).[88]

$^{31}P\{^1H\}$ and $^{19}F\{^1H\}$ NMR reaction monitoring revealed the initial formation of $PF_3$ ($\delta$ $^{19}F$ −34.5 ppm, d, $^1J_{PF}$ = 1400.9 Hz, t = 1 h),[93,94] which subsequently transforms into a mixture of P(V) species (Figure 4 and SI Section S3.19). The $^{19}F\{^1H\}$ NMR spectra showed two sets of resonances with distinct time-dependent integrals, demonstrating that they do not arise from a single compound but rather from at least two different Lewis

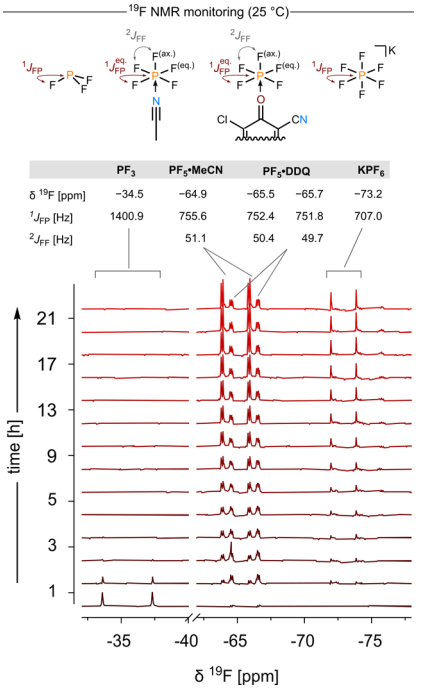


**Figure 4.** Section of the $^{19}F\{^1H\}$ NMR reaction monitoring over 23 h at 25 °C (for conditions, see Figure 3a) showing the gradual formation of $PF_3$, $PF_5$·MeCN and $KPF_6$).[96−98] For details, see SI Section S3.19.

base adducts of $PF_5$ (Figure S24). The major species was assigned as $PF_5$·MeCN, based on chemical shifts and $^1J_{PF}/^2J_{FF}$ coupling constants of the four equatorial (eq.) fluorine atoms ($\delta$ $^{19}F$ −64.9 ppm, $^1J_{PF(eq.)}$ = 755.6 Hz, $^2J_{FF}$ = 51.1 Hz) consistent with literature data.[95−100] The minor signals are doublet of doublets. These resonances are presumably attributed to DDQ adducts of $PF_5$ ($PF_5$·DDQ, $\delta$ $^{19}F$ −65.7 ppm, $^1J_{PF(eq.)}$ = 751.8 Hz, $^2J_{FF}$ = 49.7 Hz, and −65.5 ppm, $^1J_{PF(eq.)}$ = 752.4 Hz, $^2J_{FF}$ = 50.4 Hz). The observation of two sets of resonances may arise from different coordination modes or oxidation states of the quinone framework (DDQ or $DDQ^{2-}$). $KPF_6$ is slowly generated from these intermediates as the final product ($\delta$ $^{19}F$ −73.2 ppm, $^1J_{PF}$ = 707.0).[101]

## Influence of Fluoride Solubility

Next, we assessed how solvents such as tetraethylene glycol (TEG) accelerate the reaction by enhancing the solubility of KF.[102−104] $^{31}P$ and $^{19}F$ NMR spectroscopy of a reaction of $P_4$, DDQ, and KF in MeCN/TEG (9:1 v:v) at 25 °C unexpectedly revealed the formation of a $PF_5$ adduct K[$PF_5$·TEG] in 27% yield, containing a deprotonated TEG molecule coordinated to phosphorus (Figure 5a). The formation of K[$PF_5$·TEG] is evidenced by a doublet of pentets in the $^{31}P\{^1H\}$ NMR spectrum ($\delta$ $^{31}P$ −140.6 ppm, $^1J_{PF(eq.)}$ = 717.7 Hz, $^1J_{PF(ax.)}$ = 689.4 Hz) and two $^{19}F\{^1H\}$ NMR resonances observed in a 4:1 integral ratio (Figure 5b, SI Section S3.5). The equatorial fluorine atoms give rise to a doublet of doublets ($\delta$ $^{19}F^{(eq.)}$ −70.1 ppm, $^1J_{PF(eq.)}$ = 717.7 Hz, $^2J_{FF}$ = 41.5 Hz, 4F), while the axial (ax.) fluorine atom gives a doublet of pentets ($\delta$ $^{19}F^{(ax.)}$ −66.5 ppm, $^1J_{PF(ax.)}$ = 689.4 Hz, $^2J_{FF}$ = 41.4 Hz, 1F). These resonances and coupling constants are similar to literature data for $PF_5OR^-$ complexes (e.g., R = Et: $\delta$ $^{31}P$ = −141.8 ppm, $^1J_{PF(eq.)}$ = 722 Hz, $^1J_{PF(ax.)}$ = 675 Hz).[45−47] In addition, the hydropentafluorophosphate anion ($HPF_5^-$) was detected ($\delta$ $^{19}F^{(eq.)}$ −56.5 ppm, $^1J_{PF}$ = 818.1 Hz, $^2J_{HF}$ = 126.9 Hz, $^2J_{FF}$ = 42.4 Hz, 4F; $\delta$ $^{19}F^{(ax.)}$ −67.5




https://doi.org/10.1021/jacs.6c04361
J. Am. Chem. Soc. XXXX, XXX, XXX−XXX

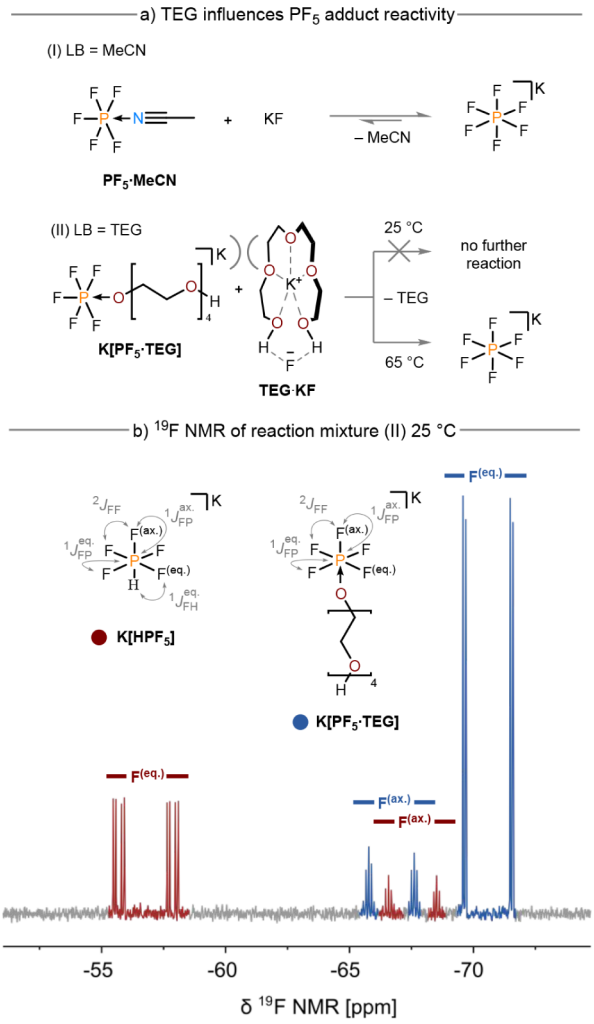


**Figure 5.** a) Rationalization for the preferential formation of the K[$PF_5$·TEG] adduct when TEG is present in the reaction mixture. b) Section of the $^{19}F\{^1H\}$ NMR spectrum of the reaction mixture of $P_4$, DDQ, and KF in MeCN/TEG (9:1) at 25 °C (Figures S47 and S48). $^{19}F$ NMR chemical shifts and coupling constants for species observed under MeCN/TEG (9:1) conditions at 25 °C: K[$PF_5$·TEG]: $\delta$ −70.1 ppm ($F^{(eq.)}$, dd, $^1J_{PF}$ = 717.7 Hz, $^2J_{FF}$ = 41.5 Hz, 4F); $\delta$ −66.5 ppm ($F^{(ax.)}$, dp, $^1J_{PF}$ = 689.4 Hz, $^2J_{FF}$ = 41.4 Hz, 1F), K[$HPF_5$]: $\delta$ −56.5 ppm ($F^{(eq.)}$, ddd, $^1J_{PF}$ = 818.1 Hz, $^2J_{HF}$ = 126.9 Hz, $^2J_{FF}$ = 42.4 Hz, 4F); $\delta$ −67.5 ppm ($F^{(ax.)}$, dp $^1J_{PF}$ = 731.1 Hz, $^2J_{FF}$ = 42.4 Hz, 1F). For further details, see SI, Section 3.5.

ppm, $^1J_{PF}$ = 731.1 Hz, $^2J_{FF}$ = 42.4 Hz, 1F) as a side product (11%) alongside trace impurities of $KPO_2F_2$ and other phosphates (<6%, see SI Section 3.5 for details).[45,105,106]

Integration of the quantitative $^{31}P\{^1H\}$ NMR spectra shows that the sum of the product integrals is significantly smaller than 100%, indicating the presence of additional NMR-silent products[92] (Figure S47). This might be attributed to polymeric and insoluble phosphorus-containing byproducts. In DCM/TEG (9:1) at 25 °C, K[$PF_5$·TEG] was obtained in 75% spectroscopic yield without the formation of K[$HPF_5$] (Figures S49 and S50).

$^{19}F$ and $^1H$ DOSY NMR experiments (see SI Section 3.21) gave additional evidence for the formation of K[$PF_5$·TEG]. The relative hydrodynamic volume of K[$PF_5$·TEG] (1,550 ± 44 Å$^3$) corresponds to the sum of the volumes of $KPF_6$ (237.9 ± 10 Å$^3$) and TEG (1,335 ± 15 Å$^3$). Electrospray ionization mass

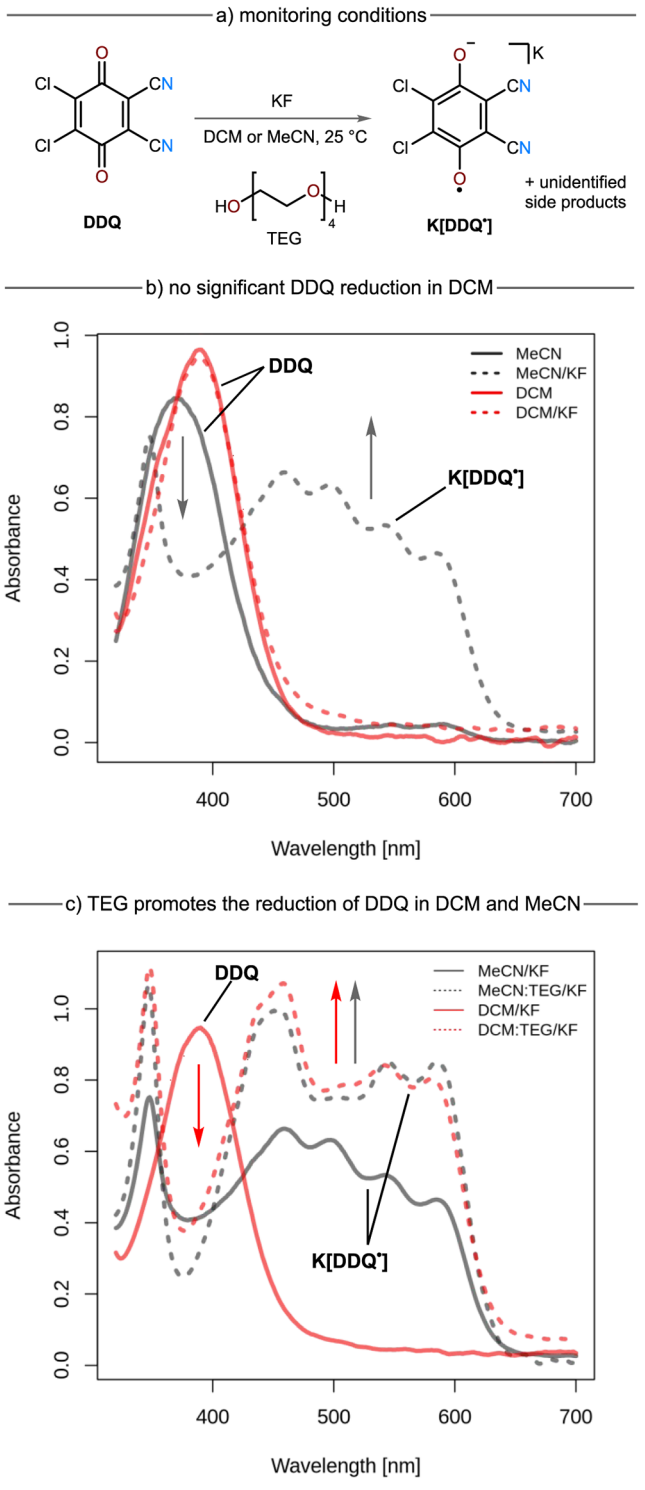


**Figure 6.** a) Schematic representation of the studied reaction. b) UV−Vis spectra of DDQ (bold lines) and DDQ with an excess of KF (dotted lines) in MeCN (black) and DCM (red), showing the generation of K[$DDQ^•$] in MeCN but not in DCM. c) UV−Vis spectra of DDQ in MeCN (black) and DCM (red) with an excess of KF added and in the presence of TEG, which enhances fluoride solubility and thus enables the reaction of DDQ and $F^-$ in DCM. This highlights that fluoride solubility is a key factor in steering the reaction outcome. For details, see Section 3.18 in the SI.

spectrometry (ESI-MS) of the reaction mixture (MeCN/TEG, 9:1, Table S15, entry 1) revealed a signal corresponding to




https://doi.org/10.1021/jacs.6c04361
J. Am. Chem. Soc. XXXX, XXX, XXX−XXX

**Scheme 3. Proposed Reaction Steps Showing the Solvent-Dependent Reactivity. In Coordinating Solvents, DDQ Can Interact with MF and Efficiently Fluorinate $P_4$ to $KPF_6$ (Pathway a, Gray). When TEG Is Present in the Reaction Mixture, the Reaction Stops at the Penultimate Step (K[$PF_5$·TEG], Blue). In Noncoordinating Solvents, such as DCM, There Is No Significant Interaction between DDQ and MF, Thus Pathway b) (Red) Becomes Dominant and the Reaction Stops at $PF_3$**

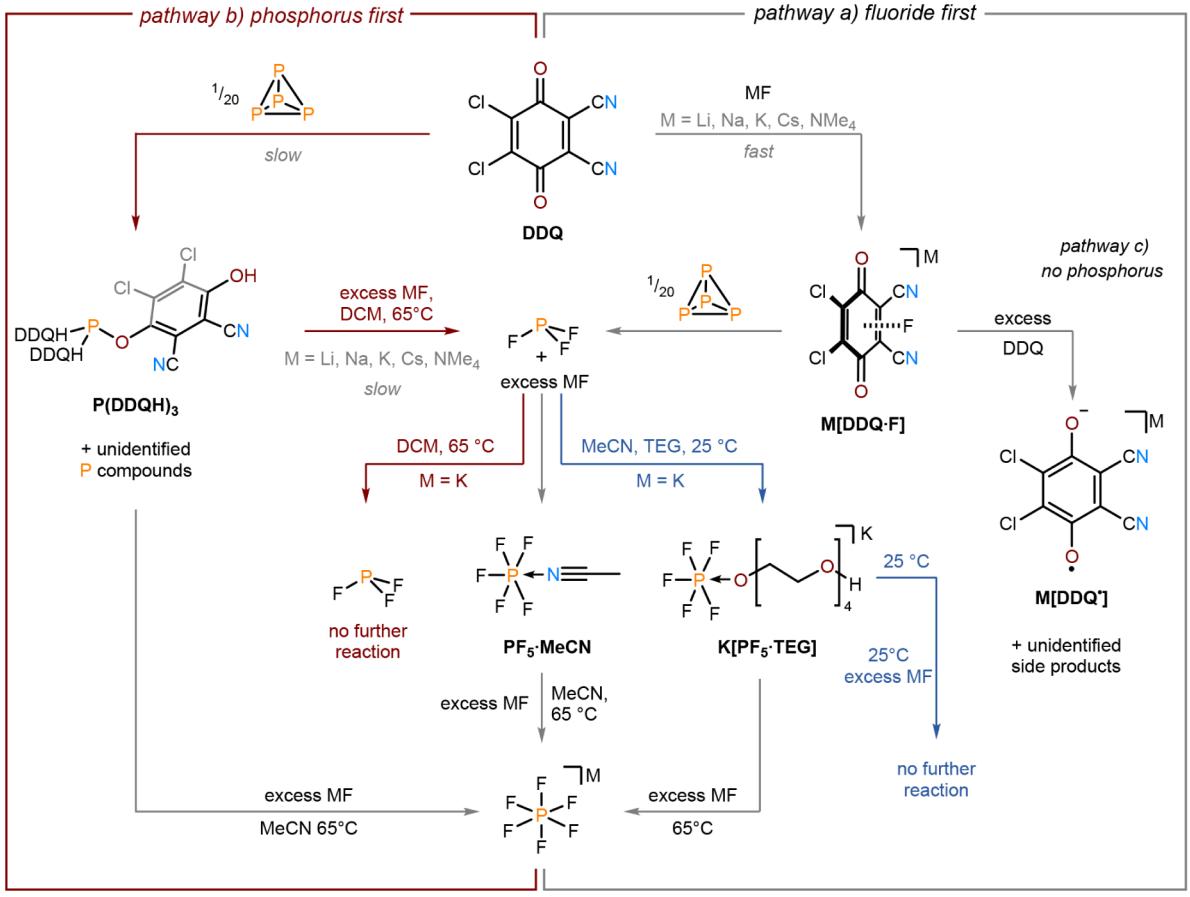


K[$PF_5$·TEG] at $m/z$ = 319.0619 (calcd: 319.0733, Figures S73 and S74).

The use of TEG as an additive affords a higher yield of fluorinated phosphorus products after 18 h (K[$PF_5$·TEG]: 75%, 25 °C) than in its absence ($KPF_6$: 41%, 25 °C), demonstrating an increased reaction rate, likely due to a higher fluoride concentration. The formation of K[$PF_5$·TEG] appears to be a kinetic phenomenon, as increasing the reaction temperature to 65 °C leads to the formation of $PF_6^-$ (Table S15, Figures S51 and S52). Presumably, TEG's chelation of fluoride impedes the final fluorination step (Figure 5a).

The product distribution is completely different when the reaction is performed in hot DCM (65 °C). In this case, $PF_3$ ($\delta$ $^{31}$P 104.6 ppm, $^1J_{PF}$ = 1400.9 Hz, Figure S4) is formed in 13% yield (65 °C, Table S3) with P(DDQH)$_3$ ($\delta$ $^{31}$P 136.5 ppm, Figure S3) being a minor side product.[92] The UV−Vis absorption spectra of DDQ and KF in DCM showed no change in absorbance, indicating that there is no reaction between DDQ and KF (Figure 6). This is likely due to the poor solubility of fluoride in DCM.[75] In contrast, analogous experiments performed using MeCN revealed the characteristic formation of $DDQ^{\cdot-}$ (presumably via M[DDQ·F], Figure 6 and Scheme 1b).[66,88] These results indicate that $P_4$ fluorination proceeds via distinct pathways in DCM and MeCN. In DCM, fluorination of $P_4$ to $PF_3$ proceeds slowly, presumably involving the phosphite P(DDQH)$_3$. Fluorination via similar DDQ-containing phosphonates has been described by Yang et al. (Scheme 1a).[49] In MeCN, DDQ-fluoride complexes of the type K[DDQ·F] are generated, which fluorinate $P_4$ to $KPF_6$.

This hypothesis is supported by investigations of the reaction between DDQ and KF using solvent mixtures of DCM and MeCN with TEG (DCM/TEG or MeCN/TEG 9:1 v:v, Figure 6c). Notably, the formation of $DDQ^{\cdot-}$ is observed by UV−Vis absorption spectroscopy in these mixtures. In contrast, in pure DCM, $DDQ^{\cdot-}$ is not detected by UV−Vis spectroscopy. The formation of $DDQ^{\cdot-}$ coincides with the formation of K[$PF_5$·TEG] in DCM/TEG and MeCN/TEG when $P_4$ is present under similar conditions (Figure 5 and SI, Section S3.5).

To test whether DDQ mainly acts by solubilizing fluoride via $\sigma$-complex formation, we employed the strong oxidant Magic Blue in the presence of crypt-222 (7.5 equiv.) as fluoride-solubilizing agent. These conditions afforded $KPF_6$ in 30% NMR yield (along with K[$HPF_5$], see Section 2.6, SI). Note that Magic Blue does not afford $KPF_6$ in the absence of cryptand (Table S10). Further investigations are needed to elucidate the mechanism of the fluorine-transfer step.

## Summary of Reaction Steps

As shown in Scheme 3, the underlying reaction pathways can be divided into two distinct "fluoride-first" and "phosphorus-first" manifolds, depending on whether the reaction is performed in coordinating or noncoordinating solvent. In the coordinating solvent MeCN, the DDQ/M[DDQ·F] mixture oxidizes and fluorinates $P_4$ to yield $PF_3$ and $PF_5$·MeCN, as observed in the


https://doi.org/10.1021/jacs.6c04361
J. Am. Chem. Soc. XXXX, XXX, XXX−XXX

NMR monitoring studies (Figure 5), which ultimately react with fluoride to form $MPF_6$ salts (Scheme 3, pathway a). In the presence of TEG, the reaction at 25 °C stops at K[$PF_5$·TEG], whereas the reaction under the same conditions at 65 °C proceeds fully to $KPF_6$, as coordination of TEG to KF hinders further reactivity kinetically (Figure 5a). In the absence of a suitable redox-active fluoride acceptor such as $P_4$, M[DDQ·F] decomposes unproductively, partially generating $DDQ^{\cdot-}$ (Scheme 3, pathway c) and other unidentified fluorinated quinone species (Figure S67).

Quinone-fluoride complexes are not formed to a significant extent in DCM (Figure 6b). In this case, DDQ reacts directly with $P_4$ to form the phosphite-like intermediate $P(DDQH)_3$ in traces (5%) among other NMR-silent phosphorus species, which remain active in the fluorination (Scheme 2). Reaction with fluoride in DCM subsequently generates $PF_3$ (Scheme 3, pathway b, SI Section 3.14). $P(DDQH)_3$ was not detected in $^{31}P\{^1H\}$ NMR monitoring studies in MeCN (Figures 4 and S68−72), suggesting that it does not contribute significantly to $PF_6^-$ formation, even though species related to $P(DDQH)_3$ have been proposed as intermediates in the fluorination of phosphonates.[49]

## CONCLUSIONS

This work reports the synthesis of $PF_6^-$ salts directly from $P_4$ using commercial electron-deficient quinonoid oxidants and simple fluoride sources under mild conditions. To our knowledge, this is the first direct oxidative fluorination of $P_4$, avoiding the use of chlorinated intermediates derived from $Cl_2$ gas or $Cl_2$-surrogates. Systematic variation of reaction parameters allowed the targeted generation of $PF_3$, K[$PF_5$·TEG], and $MPF_6$ salts (M = Li, Na, K, Cs, $NMe_4$). Studies of model reaction sequences identified transient donor−acceptor interactions (M[DDQ·F]) as key to increasing the effective fluoride concentration and promoting oxidative fluorination.[66] Solvents with low fluoride solubility, such as DCM, redirect the reaction to form $P(DDQH)_3$ in traces, among other P-species undetectable by NMR, which produce $PF_3$ through nucleophilic substitution. Adding TEG to MeCN or DCM improves KF solubility, allowing the formation of K[$PF_5$·TEG] while preventing further fluorination at room temperature. Detailed NMR and UV−Vis monitoring studies reveal $PF_3$ and $PF_5$·MeCN as intermediates en route to $PF_6^-$ and show that DDQ simultaneously acts as a single-electron oxidant and fluoride-ion shuttle.

Our results reveal a promising new avenue for converting $P_4$ into valuable phosphorus fluorides via simple one-pot procedures. Additionally, we demonstrate the deliberate use of quinones for oxidative fluorination, broadening the synthetic scope of quinonoid oxidants in fluorine chemistry.

Future work in our laboratory will examine catalytic routes to $PF_6^-$ and $PF_5$·LB species using the fluorination strategy outlined in this work, including the development of electrochemical methods. Furthermore, it seems likely that $P_4$ activation by quinones can be used for the synthesis of other valuable phosphorus compounds via nucleophilic substitution. Additionally, transiently formed complexes such as K[DDQ·F] could serve as versatile fluorination reagents in other synthetic contexts.

## ASSOCIATED CONTENT

### Supporting Information

The Supporting Information is available free of charge at https://pubs.acs.org/doi/10.1021/jacs.6c04361.

Methods, experimental procedures, reaction optimization, scale-up and product isolation, analytical data including NMR, UV−Vis and ESI-MS spectra DOSY NMR, and spectroelectrochemistry data (PDF)

## AUTHOR INFORMATION


### Corresponding Authors

**Robert Wolf** − *Institute of Inorganic Chemistry, University of Regensburg, Regensburg 93040, Germany;* orcid.org/0000-0003-4066-6483; Email: robert.wolf@ur.de

**Rafael E. Rodríguez-Lugo** − *Institute of Inorganic Chemistry, University of Regensburg, Regensburg 93040, Germany;* Present Address: Istituto di Chimica dei Composti Organometallici, 50019 Sesto Fiorentino, Italy; orcid.org/0000-0002-1317-2640; Email: rafael.rodriguez@iccom.cnr.it

### Authors

**Benjamin Falge** − *Institute of Inorganic Chemistry, University of Regensburg, Regensburg 93040, Germany*

**Maximilian Philipp** − *Institute of Organic Chemistry, University of Regensburg, Regensburg 93040, Germany;* orcid.org/0009-0003-5428-6251

**Tobias Villing** − *Institute of Inorganic Chemistry, University of Regensburg, Regensburg 93040, Germany*

**Ruth M. Gschwind** − *Institute of Organic Chemistry, University of Regensburg, Regensburg 93040, Germany;* orcid.org/0000-0003-3052-0077

Complete contact information is available at: https://pubs.acs.org/10.1021/jacs.6c04361


### Author Contributions

The manuscript was written through contributions of all authors. All authors have given approval to the final version of the manuscript.

### Notes

The authors declare the following competing financial interest(s): A patent relating to the work described herein has been filed by RR, RW and the University of Regensburg (EP 23152063.6-1108). The authors declare no other conflicts of interest.

## ACKNOWLEDGMENTS

We thank Olivia Sealy for her experimental assistance and Dr. Gábor Balázs for stimulating discussions. We gratefully acknowledge financial support by the Deutsche Forschungsgemeinschaft (WO 1496/12-1, project number 548830090). B.F. and M.P. are members of the Elite Network of Bavaria International Doctorate Program of Excellence: 'Photo-Electro Catalysis'.

## REFERENCES

(1) Gouverneur, V.; Seppelt, K. Introduction: Fluorine Chemistry. *Chem. Rev.* **2015**, *115* (2), 563−565.

(2) Magre, M.; Ni, S.; Cornella, J. (Hetero)Aryl-SVI Fluorides: Synthetic Development and Opportunities. *Angew. Chem., Int. Ed.* **2022**, *61* (23), No. e202200904.

(3) Wang, M.; Ruskin, J.; Marques, J.; Garrison, N.; Lectka, T. Selective Fluorination of Complex Molecules: Late-Stage Functionalization. *Chem. Rev.* **2025**, *125* (19), 9382−9428.
(4) Fujiwara, T.; O'Hagan, D. Successful Fluorine-Containing Herbicide Agrochemicals. *J. Fluor. Chem.* **2014**, *167*, 16−29.
(5) Jeschke, P. Current Trends in the Design of Fluorine-Containing Agrochemicals. In *Organofluorine Chemistry*; John Wiley & Sons, Ltd., 2021; pp. 363−395.
(6) Pagliaro, M.; Ciriminna, R. New Fluorinated Functional Materials. *J. Mater. Chem.* **2005**, *15* (47), 4981−4991.
(7) Liu, S.; Zhou, J.; Yu, L.; Liu, Y.; Huang, Y.; Ouyang, Y.; Liu, G.-K.; Xu, X.-H.; Shibata, N. Nitrogen-Based Organofluorine Functional Molecules: Synthesis and Applications. *Chem. Rev.* **2025**, *125* (9), 4603−4764.
(8) Wang, Y.; Yang, X.; Meng, Y.; Wen, Z.; Han, R.; Hu, X.; Sun, B.; Kang, F.; Li, B.; Zhou, D.; Wang, C.; Wang, G. Fluorine Chemistry in Rechargeable Batteries: Challenges, Progress, and Perspectives. *Chem. Rev.* **2024**, *124* (6), 3494−3589.
(9) Yuan, D.; He, Y.; Sun, X.; Li, Z.; Li, B.; Yang, K. Recent Advances in the Application of Selectfluor as a Versatile Reactant in Organic Photo- and Electrochemical Synthesis. *ChemistrySelect* **2025**, *10* (7), No. e202405859.
(10) Fuchigami, T.; Inagi, S. Selective Electrochemical Fluorination of Organic Molecules and Macromolecules in Ionic Liquids. *Chem. Commun.* **2011**, *47* (37), 10211−10223.
(11) Ye, C.; Twamley, B.; Shreeve, J. M. Straightforward Syntheses of Hypervalent Iodine(III) Reagents Mediated by Selectfluor. *Org. Lett.* **2005**, *7* (18), 3961−3964.
(12) Hart, M. A.; Uhlenbruck, B. J. H.; Levy, J. N.; McNally, A. 3-Selective Pyridine Fluorination via Zincke Imine Intermediates. *J. Am. Chem. Soc.* **2025**, *147*, 18406.
(13) Sweeting, S. G.; Lennox, A. J. J. Non-Aqueous Binary and Ternary nHF·Base Fluoride Reagents: Characterization of Structure, Properties, and Reactivity. *J. Am. Chem. Soc.* **2025**, *147*, 19329.
(14) Kraemer, Y.; Bergman, E. N.; Togni, A.; Pitts, C. R. Oxidative Fluorination of Heteroatoms Enabled by Trichloroisocyanuric Acid and Potassium Fluoride. *Angew. Chem., Int. Ed.* **2022**, *61* (31), No. e202205088.
(15) Dean, A. C.; Randle, E. H.; Lacey, A. J. D.; Marczak Giorio, G. A.; Doobary, S.; Cons, B. D.; Lennox, A. J. J. Alkene 1,3-Difluorination via Transient Oxonium Intermediates. *Angew. Chem., Int. Ed.* **2024**, *63* (30), No. e202404666.
(16) Han, Z.-Z.; Zhang, C.-P. Fluorination and Fluoroalkylation Reactions Mediated by Hypervalent Iodine Reagents. *Adv. Synth. Catal.* **2020**, *362* (20), 4256−4292.
(17) Kitamura, T.; Oyamada, J.; Higashi, M.; Kishikawa, Y. Molecular Iodine as a Catalyst for Alkene Difluorination. *J. Org. Chem.* **2024**, *89*, 5896.
(18) Liu, W.; Groves, J. T. Manganese Catalyzed C−H Halogenation. *Acc. Chem. Res.* **2015**, *48* (6), 1727−1735.
(19) Marchese, A. D.; Adrianov, T.; Lautens, M. Recent Strategies for Carbon−Halogen Bond Formation Using Nickel. *Angew. Chem., Int. Ed.* **2021**, *60* (31), 16750−16762.
(20) Leszczynski, P. J.; Jadwiszczak, M. J.; Grochala, W. Application of Silver Compounds in Fluoroorganic Synthesis: A Minireview. *ChemistrySelect* **2023**, *8* (25), No. e202301775.
(21) Fuchigami, T.; Inagi, S. Recent Advances in Electrochemical Systems for Selective Fluorination of Organic Compounds. *Acc. Chem. Res.* **2020**, *53* (2), 322−334.
(22) Li, B.; Xu, M.; Feng, P.; Xu, S. Electrochemical Construction of C−F Bonds: Recent Advances and Future Perspectives. *Eur. J. Org. Chem.* **2024**, *27* (39), No. e202400605.
(23) Thadathil, D. A.; Varghese, A.; Radhakrishnan, K. V. Review—Electrochemical Strategies for Selective Fluorination of Organic Compounds. *J. Electrochem. Soc.* **2021**, *168* (7), 075503.
(24) Nitta, N.; Wu, F.; Lee, J. T.; Yushin, G. Li-Ion Battery Materials: Present and Future. *Mater. Today Commun.* **2015**, *18* (5), 252−264.
(25) Manthiram, A. An Outlook on Lithium Ion Battery Technology. *ACS Cent. Sci.* **2017**, *3* (10), 1063−1069.
(26) Manthiram, A. A Reflection on Lithium-Ion Battery Cathode Chemistry. *Nat. Commun.* **2020**, *11* (1), 1550.
(27) Chen, Y.; Kang, Y.; Zhao, Y.; Wang, L.; Liu, J.; Li, Y.; Liang, Z.; He, X.; Li, X.; Tavajohi, N.; Li, B. A Review of Lithium-Ion Battery Safety Concerns: The Issues, Strategies, and Testing Standards. *J. Energy Chem.* **2021**, *59*, 83−99.
(28) *Electrolytes for Lithium and Lithium-Ion Batteries*, Jow, T. R.; Xu, K.; Borodin, O.; Ue, M., 1st ed.; Springer: New York, NY, 2014; Vol. *58*.
(29) Qian, Y.; Hu, S.; Zou, X.; Deng, Z.; Xu, Y.; Cao, Z.; Kang, Y.; Deng, Y.; Shi, Q.; Xu, K.; Deng, Y. How Electrolyte Additives Work in Li-Ion Batteries. *Energy Storage Mater.* **2019**, *20*, 208−215.
(30) Goodenough, J. B.; Kim, Y. Challenges for Rechargeable Li Batteries. *Chem. Mater.* **2010**, *22* (3), 587−603.
(31) Zubi, G.; Dufo-López, R.; Carvalho, M.; Pasaoglu, G. The Lithium-Ion Battery: State of the Art and Future Perspectives. *Renew. Sustain. Energy Rev.* **2018**, *89*, 292−308.
(32) Kominar, B.; Iacoud, M.; Joubert, P.; Bonnet, P. Synthesis of phosphorus pentafluoride by fluorination of phosphorus trichloride; CN 1,188,072 A, 1998.
(33) Joubert, P.; Perdrieux, S. Industrial Method for Continuously Making a $PF_5$ and HCl Mixture and Resulting Mixture; EP 1,094,984 B1, 2019.
(34) Smagin, A. A.; Matyukha, V. A.; Korobtsev, V. P. Application of Thermogravimetric Studies for Optimization of Lithium Hexafluorophosphate Production. *J. Power Sources* **1997**, *68* (2), 326−327.
(35) Na, D.-C.; Woo, B.-W.; Park, S.-H.; Lee, J.-H. Manufacturing Method for Lithium Hexafluoro Phosphate; US 6,387,340 B1, 2002.
(36) Tsujioka, S.; Ito, H.; Takahata, M.; Kawashima, T.; Sasaki, H. Production of Lithium Hexafluorophosphate; JP 10,316,409 A, 1998.
(37) Waki, M.; Miyamoto, K.; Aoki, K. Manufacturing Method of Hexafluorophosphate; US 20,100,317,511 A1, 2013.
(38) Liu, J.; Cai, Y.; Xiao, C.; Zhang, H.; Lv, F.; Luo, C.; Hu, Z.; Cao, Y.; Cao, B.; Yu, L. Synthesis of $LiPF_6$ Using $CaF_2$ as the Fluorinating Agent Directly: An Advanced Industrial Production Process Fully Harmonious to the Environments. *Ind. Eng. Chem. Res.* **2019**, *58* (44), 20491−20494.
(39) Liu, J.; Li, X.; Wang, Z.; Guo, H.; Peng, W.; Zhang, Y.; Hu, Q. Preparation and Characterization of Lithium Hexafluorophosphate for Lithium-Ion Battery Electrolyte. *Trans. Nonferrous Met. Soc. China* **2010**, *20* (2), 344−348.
(40) Kim, J.-H.; Nagahara, K.; Yonezawa, S.; Takashima, M. Preparation of Lithium Hexafluorophosphate from LiF and P in Fluorine Atmosphere. *Chem. Lett.* **2004**, *33* (7), 884−885.
(41) Kim, J.-H.; Yonezawa, S.; Takashima, M. Reaction between LiF and $MF_5$ (M = Ta, Nb) in a Fluorine Atmosphere. *J. Fluor. Chem.* **2006**, *127* (8), 1054−1057.
(42) Kim, J.-H.; Umeda, H.; Ohe, M.; Yonezawa, S.; Takashima, M. Preparation of Pure $LiPF_6$ Using Fluorine Gas at Room Temperature. *Chem. Lett.* **2011**, *40* (4), 360−361.
(43) Geeson, M. B.; Cummins, C. C. Phosphoric Acid as a Precursor to Chemicals Traditionally Synthesized from White Phosphorus. *Science* **2018**, *359* (6382), 1383−1385.
(44) Geeson, M. B.; Cummins, C. C. Let's Make White Phosphorus Obsolete. *ACS Cent. Sci.* **2020**, *6* (6), 848−860.
(45) Riesel, L.; Kant, M. Synthese Und Eigenschaften von Pentafluorophosphaten, $YPF_5^-$ (Y = OR, NHAr), Und $PF_5 \cdot$ Amin-Addukten, $PF_5 \cdot HNR_2$. *Z. Anorg. Allg. Chem.* **1985**, *530* (11), 207−212.
(46) Riesel, L.; Kant, M. Die Reaktion der Zweikomponentensysteme $P(OR)_{3-x}(NR_2)_x$ (x = 0−3)/$CCl_4$ und $P_4$/$CCl_4$ mit HF-Donatoren. *Z. Anorg. Allg. Chem.* **1985**, *531* (12), 73−81.
(47) Riesel, L.; Sturm, D.; Nagel, A.; Taudien, S.; Beuster, A.; Karwatzki, A. Synthese von Fluoro-$\lambda^5$-monophosphazenen und Fluoro-1,3-diaza-2$\lambda^5$, 4$\lambda^5$-diphosphetidinen mittels der Staudinger-Reaktion. *Z. Anorg. Allg. Chem.* **1986**, *542* (11), 157−166.
(48) Riesel, L.; Lindemann, D. Zum oxydativen Abbau von elementarem Phosphor, $P_4$, mit $CCl_4$ und 1,2-Dinucleophilen. *Z. Anorg. Allg. Chem.* **1991**, *606*, 219−227.




https://doi.org/10.1021/jacs.6c04361
J. Am. Chem. Soc. XXXX, XXX, XXX−XXX

(49) Liu, N.; Mao, L.-L.; Yang, B.; Yang, S.-D. Copper-Promoted Oxidative-Fluorination of Arylphosphine under Mild Conditions. *Chem. Commun.* **2014**, *50* (74), 10879−10882.
(50) Bornemann, D.; Pitts, C. R.; Wettstein, L.; Brüning, F.; Küng, S.; Guan, L.; Trapp, N.; Grützmacher, H.; Togni, A. Deoxygenative Fluorination of Phosphine Oxides: A General Route to Fluorinated Organophosphorus(V) Compounds and Beyond. *Angew. Chem., Int. Ed.* **2020**, *59* (50), 22790−22795.
(51) Bornemann, D.; Brüning, F.; Bartalucci, N.; Wettstein, L.; Pitts, C. R. Examining Trichloroisocyanuric Acid and Oxalyl Chloride in Complementary Approaches to Fluorination of Group 15 Heteroatoms. *Helv. Chim. Acta* **2021**, *104* (2), No. e2000218.
(52) Acharya, J.; Gupta, A. K.; Pardasani, D.; Dubey, D. K.; Kaushik, M. P. Trichloroisocyanuric Acid−KF as an Efficient Reagent for One-Pot Synthesis of Dialkylfluorophosphates from Dialkylphosphites. *Synth. Commun.* **2008**, *38* (21), 3760−3765.
(53) Scheer, M.; Balázs, G.; Seitz, A. $P_4$ Activation by Main Group Elements and Compounds. *Chem. Rev.* **2010**, *110* (7), 4236−4256.
(54) Hoidn, C. M.; Scott, D. J.; Wolf, R. Transition-Metal-Mediated Functionalization of White Phosphorus. *Chem. Eur. J.* **2021**, *27* (6), 1886−1902.
(55) Scott, D. J.; Cammarata, J.; Schimpf, M.; Wolf, R. Synthesis of Monophosphines Directly from White Phosphorus. *Nat. Chem.* **2021**, *13* (5), 458−464.
(56) Scott, D. J. Recent Breakthroughs in $P_4$ Chemistry: Towards Practical, Direct Transformations into $P_1$ Compounds. *Angew. Chem., Int. Ed.* **2022**, *61* (28), No. e202205019.
(57) Lennert, U.; Arockiam, P. B.; Streitferdt, V.; Scott, D. J.; Rödl, C.; Gschwind, R. M.; Wolf, R. Direct Catalytic Transformation of White Phosphorus into Arylphosphines and Phosphonium Salts. *Nat. Catal.* **2019**, *2* (12), 1101−1106.
(58) Budnikova, G.; Kargin, M.; Zaripov, I. M.; Romakhin, A. S.; Ignat'ev, A.; Nikitin, E. V.; Tomilov, A. P. Electrochemically Induced Processes of Formation of Phosphorus Acid Derivatives. 4. Synthesis of Trialkyl Phosphates from White Phosphorus. *Russ. Chem. Bull.* **1992**, *41* (9), 1585−1588.
(59) Milyukov, V. A.; Budnikova, Y. H.; Sinyashin, O. G. Organic Chemistry of Elemental Phosphorus. *Russ. Chem. Rev.* **2005**, *74* (9), 781−805.
(60) Mei, Y.; Yan, Z.; Liu, L. L. Facile Synthesis of the Dicyanophosphide Anion via Electrochemical Activation of White Phosphorus: An Avenue to Organophosphorus Compounds. *J. Am. Chem. Soc.* **2022**, *144* (4), 1517−1522.
(61) Horsley Downie, T. M.; Velić, A.; Coelho, L. A.; Wolf, R.; Scott, D. J. Closing the Loop: Low-Waste Phosphorus Functionalization Enabled by Simple Disulfides. *ChemSusChem* **2025**, *18* (7), No. e202401895.
(62) Donath, M.; Schwedtmann, K.; Schneider, T.; Hennersdorf, F.; Bauzá, A.; Frontera, A.; Weigand, J. J. Direct Conversion of White Phosphorus to Versatile Phosphorus Transfer Reagents via Oxidative Onioation. *Nat. Chem.* **2022**, *14* (4), 384−391.
(63) Reichl, S.; Mädl, E.; Riedlberger, F.; Piesch, M.; Balázs, G.; Seidl, M.; Scheer, M. Pentaphosphaferrocene-Mediated Synthesis of Asymmetric Organo-Phosphines Starting from White Phosphorus. *Nat. Commun.* **2021**, *12* (1), 5774.
(64) Heinl, S.; Reisinger, S.; Schwarzmaier, C.; Bodensteiner, M.; Scheer, M. Selective Functionalization of $P_4$ by Metal-Mediated C-P Bond Formation. *Angew. Chem., Int. Ed.* **2014**, *53* (29), 7639−7642.
(65) Cammarata, J.; Westermair, F. F.; Coburger, P.; Duvinage, D.; Janssen, M.; Uttendorfer, M. K.; Beckmann, J.; Gschwind, R. M.; Wolf, R.; Scott, D. J. Unravelling White Phosphorus: Experimental and Computational Studies Reveal the Mechanisms of $P_4$ Hydrostannylation. *Angew. Chem., Int. Ed.* **2024**, *63* (42), No. e202408423.
(66) Kepler, S.; Zeller, M.; Rosokha, S. V. Anion−$\pi$ Complexes of Halides with *p*-Benzoquinones: Structures, Thermodynamics, and Criteria of Charge Transfer to Electron Transfer Transition. *J. Am. Chem. Soc.* **2019**, *141* (23), 9338−9348.
(67) Reddy, G. S.; Schmutzler, R. $^{31}P$ and $^{19}F$ Nuclear Magnetic Resonance Studies of Phosphorus-Fluorine Compounds. *Z. Naturforsch. B* **1970**, *25* (11), 1199−1214.
(68) Campion, C. L.; Li, W.; Lucht, B. L. Thermal Decomposition of $LiPF_6$-Based Electrolytes for Lithium-Ion Batteries. *J. Electrochem. Soc.* **2005**, *152* (12), A2327.
(69) Albrecht, S.; Herrmann, E. Zum Reaktionsverhalten chlorsubstituierter Methanphosphonsäuredialkylester gegenüber Trialkylphosphiten, Dialkylphosphiten und Alkohol/Natriumalkoholat. *Z. Anorg. Allg. Chem.* **1986**, *538* (7), 207−211.
(70) Guéguen, A.; Streich, D.; He, M.; Mendez, M.; Chesneau, F. F.; Novák, P.; Berg, E. J. Decomposition of $LiPF_6$ in High Energy Lithium-Ion Batteries Studied with Online Electrochemical Mass Spectrometry. *J. Electrochem. Soc.* **2016**, *163* (6), A1095−A1100.
(71) Das, S.; Natarajan, P.; König, B. Teaching Old Compounds New Tricks: DDQ-Photocatalyzed C-H Amination of Arenes with Carbamates, Urea, and N-Heterocycles. *Chem. Eur. J.* **2017**, *23* (72), 18161−18165.
(72) Natarajan, P.; König, B. Excited-State 2,3-Dichloro-5,6-Dicyano-1,4-Benzoquinone (DDQ*) Initiated Organic Synthetic Transformations under Visible-Light Irradiation. *Eur. J. Org. Chem.* **2021**, *2021* (15), 2145−2161.
(73) Nakayama, K.; Okada, Y. Arene C−H Amination with *N*-Heteroarenes by Catalytic DDQ Photocatalysis. *J. Org. Chem.* **2023**, *88* (9), 5913−5922.
(74) Song, C.; Yi, H.; Dou, B.; Li, Y.; Singh, A. K.; Lei, A. Visible-Light-Mediated C2-Amination of Thiophenes by Using DDQ as an Organophotocatalyst. *Chem. Commun.* **2017**, *53* (26), 3689−3692.
(75) Wynn, D. The Solubility of Alkali-Metal Fluorides in Non-Aqueous Solvents with and without Crown Ethers, as Determined by Flame Emission Spectrometry. *Talanta* **1984**, *31* (11), 1036−1040.
(76) Aylward, G. H.; Findlay, T. J. V. *SI Chemical Data*, 3rd ed.; John Wiley & Sons: Brisbane, New York, Chichester, 1994.
(77) Cresswell, A. J.; Davies, S. G.; Roberts, P. M.; Thomson, J. E. Beyond the Balz−Schiemann Reaction: The Utility of Tetrafluoroborates and Boron Trifluoride as Nucleophilic Fluoride Sources. *Chem. Rev.* **2015**, *115* (2), 566−611.
(78) Connelly, N. G.; Geiger, W. E. Chemical Redox Agents for Organometallic Chemistry. *Chem. Rev.* **1996**, *96* (2), 877−910.
(79) Peover, M. E. 879. A Polarographic Investigation into the Redox Behaviour of Quinones: The Roles of Electron Affinity and Solvent. *J. Chem. Soc.* **1962**, 4540−4549.
(80) Huynh, M. T.; Anson, C. W.; Cavell, A. C.; Stahl, S. S.; Hammes-Schiffer, S. Quinone 1 $e^-$ and 2 $e^-$/2 $H^+$ Reduction Potentials: Identification and Analysis of Deviations from Systematic Scaling Relationships. *J. Am. Chem. Soc.* **2016**, *138* (49), 15903−15910.
(81) Gross-Lannert, R.; Kaim, W.; Olbrich-Deussner, B. Electron Delocalization in Molecule-Bridged Polymetallic Systems. Unique Neutral Complexes of TCNE or TCNQ and up to Four Organometallic Fragments $(C_5R_5)(CO)_2Mn$. *Inorg. Chem.* **1990**, *29* (25), 5046−5053.
(82) Place, S. D.; Kavanagh, P. Electrochemical Alcohol Oxidation Using a TEMPO Nitroxide Polymer as a Homogeneous and Surface-Confined Catalyst. *Electroanalysis* **2024**, *36* (4), No. e202300195.
(83) Quinones with a lower oxidation potential than the parent *p*-benzoquinone were classified as electron rich quinones, those with a higher oxidation potential were classified as electron deficient quinones.
(84) Jalilov, A.; Deats, S.; Albukhari, M.; Zeller, M.; Rosokha, S. V. Intermolecular Interactions between Halogen-Substituted p-Benzoquinones and Halide Anions: Anion-$\pi$ Complexes versus Halogen Bonding. *ChemPlusChem* **2020**, *85* (3), 441−449.
(85) Howe, D.; Wilson, J.; Rosokha, S. V. Solvent and Ionic Atmosphere Effects in Anion−$\pi$ Interactions: Complexes of Halide Anions with *p*-Benzoquinones. *J. Phys. Chem. A* **2022**, *126* (26), 4255−4263.
(86) Odubo, F. E.; Zeller, M.; Rosokha, S. V. Exploring the Nature of Anion−$\pi$ Interactions: Complexes of $\pi$-Acceptors with Fluoro- or Oxoanions Compared to the Associations with Halides. *J. Phys. Chem. A* **2023**, *127* (28), 5851−5859.

(87) Wilson, J.; Maxson, T.; Wright, I.; Zeller, M.; Rosokha, S. V. Diversity and Uniformity in Anion−$\pi$ Complexes of Thiocyanate with Aromatic, Olefinic and Quinoidal $\pi$-Acceptors. *Dalton Trans.* **2020**, *49* (25), 8734−8743.
(88) Miller, J. S.; Krusic, P. J.; Dixon, D. A.; Reiff, W. M.; Zhang, J. H.; Anderson, E. C.; Epstein, A. J. Radical Ion Salts of 2,3-Dichloro-5,6-Dicyanobenzoquinone and Metallocenes. A Reexamination of Their Magnetic and Spectroscopic Properties. *J. Am. Chem. Soc.* **1986**, *108* (15), 4459−4466.
(89) Ganesan, V.; Rosokha, S. V.; Kochi, J. K. Isolation of the Latent Precursor Complex in Electron-Transfer Dynamics. Intermolecular Association and Self-Exchange with Acceptor Anion Radicals. *J. Am. Chem. Soc.* **2003**, *125* (9), 2559−2571.
(90) Rosokha, S. V.; Kochi, J. K. Fresh Look at Electron-Transfer Mechanisms via the Donor/Acceptor Bindings in the Critical Encounter Complex. *Acc. Chem. Res.* **2008**, *41* (5), 641−653.
(91) The oxidants ferrocenium tetrafluoroborate ($FcBF_4$, 10%) and Selectfluor (SF, 95%, Figure 1a) successfully mediate $P_4$ fluorination despite not having a *p*-quinonoid structure. SF, a formal "$F^+$" source, gave excellent yields of $KPF_6$. However, its synthesis requires $F_2$, limiting its practicality in comparison with the simple fluorides used in this work.
(92) Paramagnetic or otherwise $^{31}P$ NMR-silent species cannot be excluded. Attempts to probe such intermediates by X-band EPR spectroscopy at room temperature and 77 K were inconclusive, as the persistent $DDQ^{\cdot-}$ radical anion, formed at least in trace amounts in all reaction mixtures, dominated the spectra.[88] Owing to the highly dynamic behavior of $DDQ^{\cdot-}$, only a broad unresolved signal without observable hyperfine splitting was detected under all conditions.[89,90]
(93) Clark, R. J.; Belefant, H.; Williamson, S. M. Phosphorus Trifluoride. In *Inorganic Syntheses*, Angelici, R. J., ed.; John Wiley & Sons: New York, 1990; Vol. *27*, pp. 310−315.
(94) Clark, R. J.; Busch, M. A. Stereochemical Studies of Metal Carbonylphosphorus Trifluoride Complexes. *Acc. Chem. Res.* **1973**, *6* (7), 246−252.
(95) The $^{19}F$ NMR signals of the associated axial fluorine atom of the $PF_5$-Lewis base Adducts, typically observed around −73.1 ppm as dp ($^1J_{PF}$ = 689.4 Hz, $^2J_{FF}$ = 41.4 Hz, see Figure 4) were not clearly visible during the in-situ reaction monitoring, as they were obscured by noise. Increasing the concentration further was not possible and increasing the number of scans yielded no noticeable improvements. For details see SI section 3.19.
(96) Dyke, J. M.; Emsley, J. W.; Greenacre, V. K.; Levason, W.; Monzittu, F. M.; Reid, G.; De Luca, G. Tertiary Phosphine and Arsine Complexes of Phosphorus Pentafluoride: Synthesis, Properties, and Electronic Structures. *Inorg. Chem.* **2020**, *59* (7), 4517−4526.
(97) Tebbe, F. N.; Muetterties, E. L. Autoionization in Complexes of Metal Pentafluorides. *Inorg. Chem.* **1967**, *6* (1), 129−132.
(98) Kolditz, L.; Beierlein, I. Zur Dissoziation von $PF_5{\cdot}CH_3CN$ und $AsF_5{\cdot}CH_3CN$ in Acetonitril. *Z. Chem.* **1967**, *7* (12), 468−469.
(99) John, K.-P.; Schmutzler, R. Chemie der Phosphorfluoride, XXXVII/Phosphorus-Fluorine Chemistry, XXXVII: $^{19}F$ Nuclear Magnetic Resonance Investigation of Phosphorus Pentafluoride-Base Complexes. *Z. Naturforsch. B* **1974**, *29* (11−12), 730−733.
(100) Webster, M. Addition Compounds of Group V Pentahalides. *Chem. Rev.* **1966**, *66* (1), 87−118.
(101) The $^{19}F$ NMR reaction monitoring in Figure 5 shows incomplete conversion to $KPF_6$. Even at 65 °C, the monitored reaction reached only about 50% yield after 23 h (Figure S23), considerably lower than the nearly quantitative yield obtained under standard conditions (Table 1, entry 1). This discrepancy is attributed to the lack of stirring during the in-situ NMR monitoring. The reaction mixture becomes highly viscous as the reaction proceeds, leading to poor signal-to-noise ratios and hindered mass transport. No viscosity change is observed in the stirred reaction or after completion under standard conditions.
(102) Sawamura, T.; Takahashi, K.; Inagi, S.; Fuchigami, T. Electrochemical Fluorination Using Alkali-Metal Fluorides. *Angew. Chem., Int. Ed.* **2012**, *51* (18), 4413−4416.
(103) Yan, H.; Oh, J.-S.; Song, C. E. A Mild and Efficient Method for the Selective Deprotection of Silyl Ethers Using KF in the Presence of Tetraethylene Glycol. *Org. Biomol. Chem.* **2011**, *9* (23), 8119−8121.
(104) Liang, S.; Hammond, G. B.; Xu, B. Hydrogen Bonding: Regulator for Nucleophilic Fluorination. *Chem. Eur. J.* **2017**, *23* (71), 17850−17861.
(105) Christe, K. O.; Dixon, D. A.; Wilson, W. W. Vibrational Spectra and Mutual Ligand Interactions in the Hydrogen-Substituted Main Group Hexafluorides $HPF_5^-$ and $HSF_5$. *J. Am. Chem. Soc.* **1994**, *116* (16), 7123−7128.
(106) Minkwitz, R.; Schneider, S.; Kornath, A. On the Reaction of Phosphorous acid with Superacids and the Crystal Structure of $H_5O_2^+SbF_6^-$ and $Me_4N^+HPF_5^-$. *Inorg. Chem.* **1998**, *37* (18), 4662−4665.




https://doi.org/10.1021/jacs.6c04361
J. Am. Chem. Soc. XXXX, XXX, XXX−XXX